JOURNAL OF
EMERGING INVESTIGATORS

Article

Locating sources of a high energy cosmic ray extensive air shower using HiSPARC data

Surayyah Amatul Aziz [1], Richard Phillips [2]

[1] Physics Department, Bordesley Green Girls' School & Sixth Form, Birmingham, UK

[2] Institute for Research in Schools, London, UK

SUMMARY

In the physics community, there is continued interest in high energy cosmic rays and their co-location to stellar sources, including to supernovae. Observational history and corresponding theories link the high energies associated with these types of cosmic rays to those produced in various latter evolution stages of stellar bodies. We hypothesize that high-energy cosmic ray air showers have a source region associated with specific stellar bodies. Here, we present our analysis of the locations of possible high-energy cosmic ray sources by using data from University of Twente cosmic ray detectors that are part of the High School Project on Astrophysics Research with Cosmics (HiSPARC) network. As an example of the potential of the HiSPARC network to aid cosmic ray source location, we analyzed event count data from a high-energy air shower recorded during the first week of January 2014. The data was then processed such that the direction of the air shower could be ascertained to provide the likely area of air shower origin. Angle and time data were then inputted in to Stellarium™, a free open-source planetarium application from which sources could be located. Our results suggest two sources are candidates for the origins of the high-energy air shower: the Cepheid variable Polaris and the binary system, Iota Ursae Majoris A. In sum, we have shown the potential of the HiSPARC network to aid location of stellar sources that may be responsible for detected cosmic air showers.

INTRODUCTION

The term "cosmic rays" describes high energy particles arriving from the cosmos to the Earth's upper atmosphere. These cosmic particles never reach the Earth's surface due to collisions with molecules higher in the atmosphere, which results in the decay of primary particles and the subsequent production of lower-energy secondary particles, known as an 'air-shower'. Such air showers can be observed by ground-based detectors with the data providing information on the nature of the stellar source and the chemical evolution of the universe (1). Air showers typically begin as photons or charged particles. Photons and charged particles interact with atomic nuclei found within the atmosphere. Photons are known to have weaker interactions than charged particles, meaning these interactions occur later and deeper within the atmosphere, closer to the Earth's surface (2). In contrast, charged particles collide earlier and higher in the atmosphere, and this is also characteristic of heavier nuclei. For air showers initiated by photons, observed secondary particles include additional photons, electrons, and positrons, and are termed "electromagnetic components" (2). Muons are also present in these showers, but since a muon is approximately 200 times heavier than an electron, much more energy is required to generate a muon-antimuon pair compared to the energy required to produce an electron-positron pair (2). Interactions between protons, neutrons, and mesons form nuclear fragments termed "hadronic components", where the lightest and most often produced meson is the pion (3). Pions are relatively unstable and quickly decay into other particles, so they themselves do not reach the Earth's surface (2). However, their decay product, muons, do reach the Earth's surface with high penetration, enabling long travelling distances of 5 to 10 km in these hadronic air showers prior to decay (2). Other particles such as protons and neutrons also reach the Earth's surface, but due to their larger mass (ten times that of a muon), their formation is infrequent (2). Therefore, the observed anatomy of a typical air shower means that cosmic ray detectors measure muons, electrons, and photons. The HiSPARC detectors used in this study specifically detect muon activity and hence make use of the hadronic and muonic components of an air shower (2, 4).

When detecting cosmic rays, several particles can be detected over time, each with very diverse origins. Many protons and other light nuclei originate from our Sun with relatively low energies ranging from mega electron volts (MeV) to giga electron-volts (GeV) per nucleon (4). The flow of these particles is referred to as solar winds and are closely monitored as they are able to disturb ground- and space-based electrical systems. Particles with energies of up to 10^{15} eV have origins mostly inside our galaxy (4). Very few particles are detected with higher energies. For example, less than one particle per square kilometer per year is observed for particle energies of around 10^{19} eV, with even less detected for energies over 10^{20} eV (4). Although physicists do not yet understand how these particles obtain such enormous energies, proposed sources include active galactic nuclei, neutron stars or supernova remnants. However, even these sources are unable to independently provide such a large amount of energy to a single particle (4).

Cosmic rays constantly react with the cosmic microwave background radiation (CMBR) until their energy falls below 10^{20} eV (4). Independent of the starting energy of the initial source particle, Greisen, Zatsepin and Kuzmin (GZK) proposed a theoretical upper limit to this process of 100 Mpc (around 3.26 x 10^{8} ly), known as the GZK limit (5). Here, Mpc refers to the unit megaparsec, where a parsec equates to 3.26 light years (ly), and a light year is the distance which light can travel in a vacuum in one year (9.46 x 10^{12} km). Although the GZK-threshold limits energies over 10^{20} eV, the Akeno Giant Air Shower Array (AGASA) study in Japan, which operated between 1993 and 2003, observed particle energies in excess of 10^{20} eV (6). This implies that sources of extremely energetic particles must exist within 100 Mpc of

Earth, but they remain elusive.

The search for such sources has proven difficult, primarily due to the limited number of detected particles with such high energies. The issue is further compounded by the action of Earth's magnetic field, which deflects the path taken by incoming high energy particles (7). Nevertheless, we can study high energy events where particles of energies equal to or above 10^{15} eV are detected, with the aim of unravelling the origins and nature of high energy cosmic rays. Such information will better inform our understanding of the evolution of stellar objects and ultimately the make-up and development of the cosmos.

In this investigation, we used data collected during the first week of January 2014 by the University of Twente from detectors within the European HiSPARC network. We aimed to locate stellar sources of high energy cosmic ray air showers by calculating the possible region within the celestial sphere from which the cosmic rays originated. Our hypothesis was that we would be able to co-locate potential cosmic ray source regions with particle energies of up to 10^{15} eV using an array of ground-based muon detectors. The initial observation of Iota Ursae Majoris A, a spectroscopic binary star, seemed to stand out as a promising source of high energy cosmic ray air showers. Such massive binary stellar systems with proximal orbits are able to exchange mass, ultimately forcing their evolution to supernovae and black holes (8). Our results also demonstrated that Polaris was an alternative viable stellar source responsible for the detected air shower. Polaris is a Cepheid variable, which is a periodically pulsating star that varies in diameter, temperature, and brightness (9). On a Hertzsprung-Russel diagram, we identified classical Cepheid stars as low luminosity supergiants, with potential to evolve into supernovae, and then into neutron stars and black holes (10). These Cepheid sources are presently considered as candidates for the high energy cosmic ray air shower studied.

RESULTS

The rationale of this project was to obtain and analyse high-energy cosmic ray data from the European HiSPARC network with the objective of determining the location of possible stellar sources (11). Event count data was acquired from the University of Twente over a 7-day period in the first week of January 2014 at muon detector stations 7001, 7002, and 7003. Event count was measured per hour with each one-hour window relating to a specific bin number. The time, in both sidereal and solar hours, was recorded and an angle of event excess (the direction in the sky with above average cosmic radiation) was determined (12). The rationale behind using sidereal time in calculations is based on the principle that, although the Earth is constantly rotating both around its own axis and around the Sun, the stars will have a slightly different position each day. To correct for this, the use of a sidereal time system, which measures the rotation of the Earth relative to the stars rather than the sun, was adopted. Where the solar day (24 h) is the time taken for the same place on the Earth to face the sun, the sidereal day (23 h 56 min 4 sec) is the time taken for the Earth to rotate 360° around its axis, or otherwise the time between successive passages of a distant star across the meridian.

A weighting factor was then applied to smooth the data and provide a continuous waveform that could be analysed

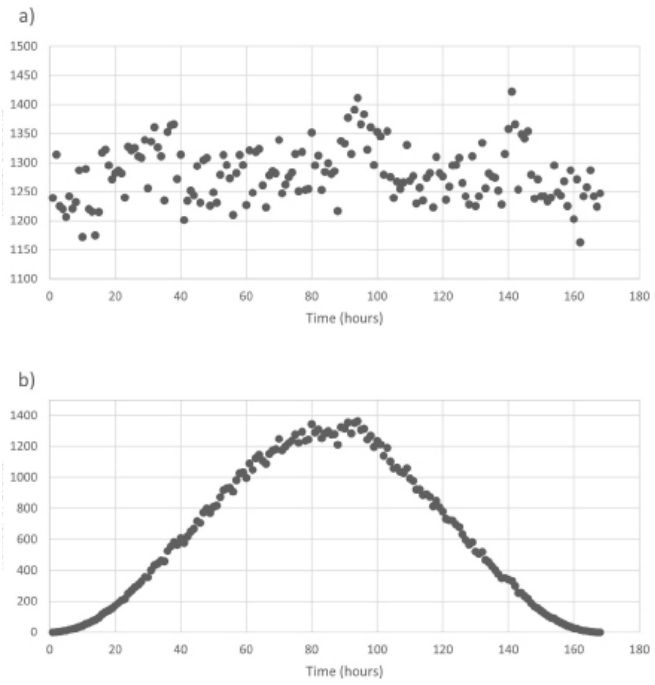

Figure 1: Events per hour data over a 7-day observation window. Events per hour data over 7 days (168 hours) were acquired (a) before, and (b) after weighting A weighting factor of ½ (1- cos (2π *b* / *B*)) was applied in (b) to allow for frequency-domain representation of the data, where *b* is the bin number of the particular reading and *B* is the total number of bins during the whole observation period. This particular weighting factor is known as a Hann window.

(Figure 1) (13, 14). The purpose of windowing is to reduce the amplitude of discontinuities at the lower and upper boundaries of the observation period under investigation to make the data easier to manipulate for further analysis (13, 14). By multiplying the time record by a finite-length window with an amplitude that varies smoothly and gradually toward zero at the edges, a continuous waveform without sharp transitions is produced. Theoretically, the weighting function should produce a pure Gaussian curve. However, as this curve is infinite and the data we used is limited to an observation period of seven days, the weighting factor applied is a spreadsheet compatible approximation of the Gaussian curve, which produced a raised cosine shape. Processing operations and calculations were performed, and processed data was then input into a Stellarium™ celestial chart with potential cosmic ray sources then lined up with the north-south meridian line on the azimuthal grid **(Appendix Table 1)** (15).

Cosmic ray events recorded by detector stations 7001, 7002, and 7003 showed direct alignment with Polaris, a classic radially pulsating Cepheid variable **(Table 1)**. Since the data was recorded in all three stations, our results suggest Polaris as the source **(Appendix Table 2-4)**. At a distance of 432.57 ly, Polaris falls within our Milky Way galaxy.

Within the data for station 7003, we also noted data supporting Iota Ursae Majoris A as a possible cosmic ray source **(Table 1)**. This binary stellar system is, at 47.33 ly, much closer to Earth compared to Polaris, but has the

Station	Possible Source	Classification	Apparent Magnitude	Right Ascension (h:min:s)	Declination (°,′,″)
7001	Polaris	Classical Cepheid	2.09	02:50:48.3	+89,19,40.4
7002	Polaris	Classical Cepheid	2.09	02:50:48.3	+89,19,40.4
7003	Polaris	Classical Cepheid	2.09	02:50:48.3	+89,19,40.4
7003	Iota Ursae Majoris A	Spectroscopic Binary	3.19	09:00:11.7	+47,58,50.6

Table 1. Observations made using celestial charts to determine potential high energy cosmic ray sources found along the North-South Meridian. The term 'right ascension' essential equates to the celestial equivalent of longitude on Earth and is commonly measured in hours, minutes, and seconds, whereas 'declination' is the celestial equivalent of latitude and is measured in degrees. Together, these two measurements allow location of a stellar object relative to the Earth.

potential for high energy cosmic ray emission. However, as event data was only captured in one out of three stations, Iota Ursae Majoris A remains a viable though weaker source target compared to Polaris.

Modelling of the data and use of the Stellarium™ celestial charts suggested that Polaris and Iota Ursae Majoris A are possible sources of the high energy cosmic rays, as observed in our observation window of week 1, January 2014.

DISCUSSION

In this investigation, our aim was to determine possible stellar origins of cosmic ray air showers observed by the European HiSPARC muon detector array. Since it is often difficult to determine the initial source location of such air showers, we hypothesized that we could define the source area by determining the celestial latitude and longitude of potential stellar objects by modelling the vertical peak incidence of an air shower.

Our analyses demonstrate that Polaris, a classical Cepheid star with a mass of 5.4 solar masses, is a recurring source within three detectors and a strong source candidate for the January 2014 cosmic air shower. Classical Cepheids are comparatively young stars; hence they are relatively higher in energy from nuclear fusion processes and are strongly concentrated in the Milky Way galaxy in clusters (15). Classical Cepheid stars are low luminosity supergiants with the potential to evolve into supernovae, and further into neutron stars and black holes, which are all thought to be very strong candidates for ultra-high energy cosmic rays (16).

An additional source we identified was Iota Ursae Majoris A, a spectroscopic binary star found using data from Station 7003. A binary star is a system of two stars that are gravitationally bound to and in orbit around each other. In binary stars, if the two stars get close enough, they gain the ability to gravitationally change each of their outer atmospheres (17). In some cases, close binary stars can exchange mass, which may bring their evolution to stages that some single stars cannot attain, such as supernovae and black holes (18).

It is worth noting that when selecting HiSPARC detector arrays for this investigation, an ideal arrangement would be a minimum of five detectors in a cluster. This arrangement would optimize detection of a high energy air shower, such as showers of secondary particles with energies above 10^{15} eV. However, due to the low probability of high energy air showers being detected, attempts of being able to download data for a high energy air shower picked up by at least five detectors was unsuccessful. During the observation window, up to three detectors at any given moment were able to record data from the same cosmic ray air shower.

If this investigation were to be repeated, there are a number of limitations from our initial study that could be addressed and mitigated to improve our experiment. These include addressing the limitations of the Stellarium™ app, increasing the observation window and/or number of detectors used, assessing detector limitations, reviewing air shower modelling assumptions and considering alternative methods of muon or cosmic ray detection.

Firstly, Stellarium™ is limited to known celestial objects, with galactic targets such as young neutron stars, pulsars, black holes and active galactic nuclei absent from the web app (16). It is possible that the located sources outlined in this investigation may not be the only sources lying within the angle in question and that they were the only sources that could be manually registered along the North-South meridian of the aximuthal grid. Use of other of planetarium apps may overcome this limitation of only using Stellarium™.

Further, increasing the observation window beyond one week would allow processing of more data over a longer period. This would provide an opportunity to investigate greater event count data and more locations with which to corroborate our suggested high energy cosmic ray sources. Increased data would also enable a better representation of the distribution of cosmic ray count across the celestial sphere and improve the precision of our results.

A limitation of using ground-based detectors such as the HiSPARC array is that the energy of the primary cosmic particle that initiates the air shower cannot be determined

directly. Instead, the energy is estimated by modelling the total amount of energy present in the different components of the cosmic air shower (i.e., muons, photons, electrons, and undetected particles). However, as it is impossible to measure every individual particle, modelling assumptions have to be adopted. One modelling assumption is that the bulk of particles travel as a thin disk in the shower front, which brings uncertainty in reconstructing shower front angles to locate sources (13). Another assumed point is that there are negligible delays in timing when the particle arrives and hits the detector, especially as the time scintillation photons take to reach the phototube depends on the distance between the phototube and the point of impact. It is also modelled that particles lose a fixed amount of energy when passing though one gram of matter (per cm^2), hence energy loss is simulated but does not factor in natural fluctuations, especially when new particles are added to the shower. Further, since the HiSPARC detectors only detect muons, much of the air shower may be missed by the detectors. This may in itself bring in possible sources of error to the methodologies implemented when researching cosmic rays via muon detection techniques, though the possible shortage of muons is difficult to quantify (2, 19). This could be a contributing factor to the scarcity of high energy events on the HiSPARC database since the interaction of primary particles with matter in the atmosphere would produce many particles through series of decay, of which only muons can be detected by HiSPARC technology (20).

Moreover, to overcome issues with modelling around muon detection, the adoption of different detection methods may be required, such as measuring Cherenkov radiation emission similar to the HiRes Fly's Eye experiment in Utah, USA, or by directly measuring the particle density using low frequency radio waves generated by electrical currents of charged particles in showers (21). Use of detectors with x-y-z co-ordinate data would also be a valuable contribution in the search for high energy cosmic ray sources, as ascertaining the direction of incoming rays would improve ability in locating the source. These include the neutrino water detector (NEVOD) of the Moscow Engineering Physics Institute and the Netherlands Low Frequency Array (LOFAR) technology (22).

Overall, though the dataset was limited, the modelling and results of sources located using the HiSPARC network are promising with a strong candidate source of Polaris. Our study showcases the possibilities for exploration and scientific endeavor in the search for celestial sources of high energy cosmic rays using a public open-source dataset. We hope our work inspires other students interested in this field to ask their own questions about the HiSPARC data and of cosmic rays in the hope that they can move the sum of our knowledge further.

MATERIALS AND METHODS

Cosmic ray event data, available on the HiSPARC public database, was initially reviewed in order to source data of high energy events, which occur simultaneously in a detector cluster location (i.e., where multiple readings of the same air shower event were taken by a number of detectors within reasonable proximity). Since the geometry of the detectors is such that they are most sensitive to secondary particles hitting from directly overhead, the method assumes that the majority of cosmic rays are from a source region perpendicular to the ground-based detector.

Event count data was selected for processing from the University of Twente cosmic ray detectors during the first week of January 2014 (01:01:2014 to 07:01:2014) at stations 7001, 7002, and 7003. Though the location and time period are limited, it allowed us to test our model and to implement the locating method using Stellarium™. Stellarium™ is a web app software that displays the sky chart of the galactic sphere (16). As well as event count data, other data available on the website from the selected detectors included pulseheight, pulseintegral, singles per second above and below threshold, and single rate above and below threshold.

Data downloaded from the HiSPARC public open-source database was inputted into a Microsoft Excel spreadsheet using a sidereal time system in calculations. The sky was then divided into four quadrants and the number of cosmic rays coming from each quadrant determined by applying simple vector decomposition. The sidereal time was then used to ascertain the angle of event excess (α) of the air shower in question, which allowed for the determination of the direction in the sky of excess (above average) cosmic rays (12). This was then converted to time in solar hours after midnight on the first day of the observation period. This allowed for observation of possible sources on the Meridian of the azimuthal grid of the sky at this time in the location of the detector.

Event count data was the weighted, using the Hann windowing function. Following the weighting of the data, a simple Fourier Transform was applied to convert into a periodic format. The Fourier transform is a mathematical function that allows for the resolution of angle data into the sum of its constituent sine and cosine functions. Graphs were constructed from the unweighted and weighted data to visually represent the effect of applying the Fourier Transform. The data was then assigned to the quadrant in which the angle (α) existed, and trigonometric principles were used to calculate the specific value of α. For ease of input into Stellarium™, α was converted back into time, specifically solar hours after midnight on the first day of the chosen observation period.

Upon ascertaining values for solar hours after midnight for each station, this value and the location of the detectors was inputted into Stellarium™. Display of the azimuthal grid enabled location of potential sources of the high-energy air shower along the North-South meridian, which is the hypothetical line in astronomy upon which the observer's zenith is joint with the North and South celestial poles. Observations made using the sky charts on Stellarium™ were therefore used to identify potential sources of high energy cosmic rays.

ACKNOWLEDGEMENTS

S.A. thanks Mr. S.S. Dhaliwal and the Institute for Research in Schools (IRIS) for providing the opportunity to access the High School Project on Astrophysics Research with Cosmics (HiSPARC). S.A. is also grateful to IRIS for recognizing her work in their annual IRIS Awards (2022). IRIS works with schools across the United Kingdom to provide opportunities for school pupils aged 12–18 to participate in STEM research and collaborate with universities and scientific institutions.

Received: September 27, 2022
Accepted: August 14, 2023

Published: October 19, 2023

REFERENCES

1. "Cosmic Rays." Institute of Physics, www.iop.org/explore-physics/understanding-our-environment/cosmic-rays. Accessed 30 Mar. 2022.
2. Kortland, Koos. "Air Showers." HiSPARC Nekhef, 2012, docs.hisparc.nl/routenet/en/Air_Showers.pdf.
3. "Particle Classification." The University of Tennessee Knoxville, electron6.phys.utk.edu/phys250/modules/module%206/particle_classification.htm. Accessed 30 Mar. 2022.
4. Kortland, Koos. "Sources of Cosmic Radiation." HiSPARC Nikhef, 2015, docs.hisparc.nl/routenet/en/Sources_of_Cosmic_Radiation.pdf.
5. Zatsepin, Georgii T., et al. "Upper Limit of the Spectrum of Cosmic Rays." Journal of Experimental and Theoretical Physics Letters, vol. 4,1966, www.jetpletters.ru/ps/1624/article_24846.shtml.
6. Takeda, Masahiro., et al. "Energy determination in the Akeno Giant Air Shower Array experiment." Astroparticle Physics, vol. 19, 2003, doi.org/10.1016/S0927-6505(02)00243-8.
7. Osinga, Gerard. "An introduction to cosmic radiation and HiSPARC." Original Dutch text Heesbeen, Cor., Morsing, Connie., Colle, Jef., Timmermans, Charles.; translated by Kaj Schadenberg, HiSPARC Nikhef, 2010, physicsatbcs.weebly.com/uploads/1/9/0/3/19039659/introduction_to_cosmic_radiation_and_hisparc.pdf.
8. "Binary Star Systems: Classification and Evolution." Space. www.space.com/22509-binary-stars.html. Accessed 30 Mar. 2022.
9. Turner, David G. "The PL calibration for Milky Way Cepheids and its implications for the distance scale." Astrophysics and Space Science, vol. 326, 2010, doi.org/10.1007/s10509-009-0258-5.
10. "Classical Cepheid." Oxford Reference, www.oxfordreference.com/view/10.1093/oi/authority.20110803095615778. Accessed 30 Mar. 2022.
11. "List of HiSPARC Stations." HiSPARC, data.hisparc.nl/show/stations_by_country/. Accessed 30 Mar. 2022.
12. Anderson, Lewis. "Locating the Source of Cosmic Rays using HiSPARC Data." STEM Activities, University of Birmingham, 2014, www.birmingham.ac.uk/Documents/college-eps/college/stem/Activities/STEM-Summer-Placement-Scheme/Final-report---Lewis-Anderson.pdf. Accessed 14 Mar. 2023.
13. Fokkema, David R.A. "The HiSPARC Cosmic Ray Experiment: Data Acquisition and Reconstruction of Shower Direction." PhD thesis, Universiteit Twente, Netherlands, 2012, doi.org/10.3990/1.9789036534383.
14. Pavlidou, Maria. "HiSPARC – How to analyse data." University of Birmingham, 2016. www.birmingham.ac.uk/Documents/college-eps/physics/outreach-documents/educators-and-general-public-documents/ASE-2016/HiSPARC-How-to-analyse-data-2017.pdf.
15. Groenewegen, Martin A.T. "Analysing the spectral energy distributions of Galactic classical Cepheids." Astronomy and Astrophysics (A&A), vol. 635, The European Southern Observatory (ESO), March. 2020, doi.org/10.1051/0004-6361/201937060
16. "Stellarium." 2021. Stellarium Web. stellarium-web.org/. Accessed 30 Mar. 2022.
17. Wilson, Robert E., Sofia, Sabatino. "Effects of tidal distortion on binary-star velocity curves and ellipsoidal variation." Astrophysics Journal, vol. 203, The American Astronomical Society, Jan. 1976, doi.org/10.1086/154062.
18. Cehula, Jakub, and Ondřej Pejcha. "A Theory of Mass Transfer in Binary Stars." Monthly Notices of the Royal Astronomical Society, vol. 524, Royal Astronomical Society, Jun. 2023, doi.org/10.1093/mnras/stad1862.
19. Albrecht, Johannes. "The Muon Puzzle in cosmic-ray induced air showers and its connection to the Large Hadron Collider." Astrophysics and Space Science, vol. 367, 2022, doi.org/10.1007/s10509-022-04054-5.
20. "The Standard Model". CERN. www.home.cern/science/physics/standard-model. Accessed 30 Mar. 2022.
21. Bird, David J. "The High Resolution (HiRes) Fly's Eye Detector." Shapiro, M.M., Silberberg, R., Wefel, J.P. (eds) Currents in High-Energy Astrophysics. NATO ASI Series, vol. 458. Springer, Dordrecht. 1995, doi.org/10.1007/978-94-011-0253-7_11.
22. "Coordinate detector for horizontal cosmic ray flux investigations." CORDIS. cordis.europa.eu/project/id/INTAS-RFBR95-0703. Accessed 30 Mar. 2022.

Appendix

Formula #	Operation	Returned Value	Elaboration on Returned Value
	Downloaded from HiSPARC Database:	Date	Date of Observation
		Time/hours	Time in hours from beginning of date of observation
		Overall bin number	The binary number starting from 1 and increasing by 1 all the way through the whole observational period
		Events per hour	Number of cosmic ray particles detected per hour
1	Overall Bin Number – 0.5	Time (Solar Hours)	Time in solar hours, increasing periodically from start of observation period
2	Time in Solar Hours * (Ratio of Days in Solar Year to Days in Sidereal Year)	Time (Sidereal Hours)	Time in sidereal hours, from start of observation period
3	Time in Solar Hours / (24* Ratio of Days in Solar Year to Days in Sidereal Year)	Number of Earth Revolutions	Number of times Earth has rotated on its axis
4	2*π*Number of Earth Revolutions	Angle (α) (Radians)	How much the earth has rotated for each bin
5	Remainder of Angle (α) / 2π	Angle (α) (Radians 0-2π)	Earth's rotation for each bin restricted between 0 and 2π radians degrees
6	½ (1- cos (2π*Bin Number of Particular Reading / Total Number of Bins During Whole Observation Period))	Weighting Factor	Hann window = weighting factor 1/2 (1-cos(2πb/B))
7	Weighting Factor * Events per Hour	Weighted Data	Weighted data, where amplitude of discontinuities at the lower and upper boundaries of observation period are reduced
8	Weighted Data * Cos (Angle (α) 0-2π)	Data x	Cosine component of weighted data
9	Weighted Data * Sin (Angle (α) 0-2π)	Data y	Sine component of weighted data
10	Sum of Weighted Data	Sum of Weighted Data	Total of weighted data
11	Sum of Data x	Sum of Data x	Total of cosine component of weighted data
12	Sum of Data y	Sum of Data y	Total of sine component of weighted data
13	$(\sqrt{[(\Sigma \text{ data x})^2 + (\Sigma \text{ data y})^2]} / \Sigma$ weighted data)*100	Percentage Deviation (of Data x and Data y from Weighted Data)	Formula deduced from Pythagorean theorem
14	Sum of Data y / Sum of Data x	Tan (α)	Based on principle that tan (α) = sin (α) / cos (α)
15	Inverse Tan [Tan (α)]	Angle (α) (Radians)	Right ascension in radians

16	Angle (α) (Rads) * 180 / π	Angle (α) (Degrees)	Right ascension in degrees
17	Angle (α) (Degrees) / 360	Fraction of Earth Revolution	Right ascension as fraction of earth revolution
18	24 * Fraction of Earth Revolution	Solar Hours after Midnight on First Day of Observation Period	Decimal format of solar hours after midnight on first day of chosen observation period

Table 1. Summary of data processing and subsequent calculations. The first column labelled “Operation” refers to the operation present in our analysis. The second column labelled “Returned Value” explains what information is gained from this operation. The third column “Elaboration on Returned Value” further describes the purpose of the returned value and why this information is useful within our wider data processing.

Enschede Station 7001 – Processed Data

Date	Time (hours)	Overall Bin Number	Events (per hour)	Time (solar hours)	Time (sidereal hours)	Number of Earth Revs	Angle, α (Rads)	Angle, α (Rads, 0-2π)	Weighting Factor	Weighted Data	Data x (cos)	Data y (sin)
01/01/2014	0	1	1239	0.50	0.50	0.02	0.13	0.13	0.00	0.43	0.43	0.06
01/01/2014	1	2	1314	1.50	1.50	0.06	0.39	0.39	0.00	1.84	1.70	0.70
01/01/2014	2	3	1225	2.50	2.49	0.10	0.66	0.66	0.00	3.85	3.05	2.35
01/01/2014	3	4	1220	3.50	3.49	0.15	0.92	0.92	0.01	6.81	4.13	5.42
01/01/2014	4	5	1207	4.50	4.49	0.19	1.18	1.18	0.01	10.52	3.99	9.73
01/01/2014	5	6	1242	5.50	5.48	0.23	1.44	1.44	0.01	15.57	1.97	15.44
01/01/2014	6	7	1221	6.50	6.48	0.27	1.71	1.71	0.02	20.80	-2.81	20.61
01/01/2014	7	8	1232	7.50	7.48	0.31	1.97	1.97	0.02	27.37	-10.61	25.23
01/01/2014	8	9	1287	8.50	8.48	0.36	2.23	2.23	0.03	36.11	-22.16	28.51
01/01/2014	9	10	1172	9.50	9.47	0.40	2.49	2.49	0.03	40.51	-32.30	24.44
01/01/2014	10	11	1289	10.50	10.47	0.44	2.76	2.76	0.04	53.78	-49.84	20.20
01/01/2014	11	12	1220	11.50	11.47	0.48	3.02	3.02	0.05	60.41	-59.96	7.39
01/01/2014	12	13	1216	12.50	12.47	0.52	3.28	3.28	0.06	70.46	-69.77	-9.82
01/01/2014	13	14	1175	13.50	13.46	0.56	3.54	3.54	0.07	78.71	-72.42	-30.82
01/01/2014	14	15	1215	14.50	14.46	0.61	3.81	3.81	0.08	93.12	-73.28	-57.45
01/01/2014	15	16	1317	15.50	15.46	0.65	4.07	4.07	0.09	114.42	-68.64	-91.55
01/01/2014	16	17	1322	16.50	16.45	0.69	4.33	4.33	0.10	129.16	-48.01	-119.91
01/01/2014	17	18	1295	17.50	17.45	0.73	4.59	4.59	0.11	141.26	-16.68	-140.28
01/01/2014	18	19	1271	18.50	18.45	0.77	4.86	4.86	0.12	153.81	22.10	-152.21
01/01/2014	19	20	1282	19.50	19.45	0.81	5.12	5.12	0.13	171.11	67.69	-157.16
01/01/2014	20	21	1287	20.50	20.44	0.86	5.38	5.38	0.15	188.48	116.92	-147.83
01/01/2014	21	22	1281	21.50	21.44	0.90	5.64	5.64	0.16	204.85	164.42	-122.19
01/01/2014	22	23	1240	22.50	22.44	0.94	5.91	5.91	0.17	215.58	200.48	-79.28
01/01/2014	23	24	1327	23.50	23.44	0.98	6.17	6.17	0.19	249.81	248.19	-28.43
02/01/2014	0	25	1321	24.50	24.43	1.02	6.43	0.15	0.20	268.28	265.33	39.68
02/01/2014	1	26	1325	25.50	25.43	1.07	6.69	0.41	0.22	289.30	265.21	115.58
02/01/2014	2	27	1311	26.50	26.43	1.11	6.96	0.67	0.23	306.75	239.77	191.33
02/01/2014	3	28	1308	27.50	27.42	1.15	7.22	0.94	0.25	327.00	193.91	263.30
02/01/2014	4	29	1339	28.50	28.42	1.19	7.48	1.20	0.27	356.66	129.73	332.23
02/01/2014	5	30	1256	29.50	29.42	1.23	7.74	1.46	0.28	355.52	38.94	353.38
02/01/2014	6	31	1336	30.50	30.42	1.27	8.01	1.72	0.30	400.87	-61.00	396.20
02/01/2014	7	32	1361	31.50	31.41	1.32	8.27	1.99	0.32	431.89	-174.24	395.18
02/01/2014	8	33	1326	32.50	32.41	1.36	8.53	2.25	0.33	444.02	-278.44	345.88
02/01/2014	9	34	1311	33.50	33.41	1.40	8.79	2.51	0.35	462.29	-373.41	272.54
02/01/2014	10	35	1235	34.50	34.41	1.44	9.06	2.77	0.37	457.68	-427.04	164.64
02/01/2014	11	36	1353	35.50	35.40	1.48	9.32	3.04	0.39	525.96	-523.04	55.36

02/01/2014	12	37	1364	36.50	36.40	1.52	9.58	3.30	0.41	555.21	-548.37	-86.84
02/01/2014	13	38	1366	37.50	37.40	1.57	9.84	3.56	0.43	581.20	-530.79	-236.77
02/01/2014	14	39	1272	38.50	38.39	1.61	10.11	3.82	0.44	564.79	-438.42	-356.06
02/01/2014	15	40	1314	39.50	39.39	1.65	10.37	4.09	0.46	607.90	-356.27	-492.56
02/01/2014	16	41	1201	40.50	40.39	1.69	10.63	4.35	0.48	578.05	-205.61	-540.24
02/01/2014	17	42	1234	41.50	41.39	1.73	10.89	4.61	0.50	617.00	-62.31	-613.85
02/01/2014	18	43	1252	42.50	42.38	1.78	11.16	4.87	0.52	649.41	104.34	-640.97
02/01/2014	19	44	1244	43.50	43.38	1.82	11.42	5.14	0.54	668.48	274.95	-609.32
02/01/2014	20	45	1294	44.50	44.38	1.86	11.68	5.40	0.56	719.44	455.95	-556.51
02/01/2014	21	46	1231	45.50	45.38	1.90	11.94	5.66	0.57	707.24	574.83	-412.01
02/01/2014	22	47	1304	46.50	46.37	1.94	12.21	5.92	0.59	773.21	723.82	-271.93
02/01/2014	23	48	1308	47.50	47.37	1.98	12.47	6.19	0.61	799.53	795.78	-77.32
03/01/2014	0	49	1226	48.50	48.37	2.03	12.73	0.17	0.63	771.66	761.09	127.25
03/01/2014	1	50	1249	49.50	49.36	2.07	12.99	0.43	0.65	808.57	735.58	335.73
03/01/2014	2	51	1231	50.50	50.36	2.11	13.26	0.69	0.67	818.79	631.12	521.63
03/01/2014	3	52	1279	51.50	51.36	2.15	13.52	0.95	0.68	873.14	505.60	711.85
03/01/2014	4	53	1313	52.50	52.36	2.19	13.78	1.22	0.70	919.03	319.50	861.70
03/01/2014	5	54	1296	53.50	53.35	2.24	14.04	1.48	0.72	929.16	85.87	925.18
03/01/2014	6	55	1273	54.50	54.35	2.28	14.31	1.74	0.73	933.92	-157.97	920.46
03/01/2014	7	56	1210	55.50	55.35	2.32	14.57	2.00	0.75	907.50	-380.36	823.95
03/01/2014	8	57	1282	56.50	56.35	2.36	14.83	2.27	0.77	982.03	-628.88	754.26
03/01/2014	9	58	1313	57.50	57.34	2.40	15.09	2.53	0.78	1026.32	-839.29	590.70
03/01/2014	10	59	1296	58.50	58.34	2.44	15.36	2.79	0.80	1032.80	-969.91	354.89
03/01/2014	11	60	1227	59.50	59.34	2.49	15.62	3.05	0.81	996.01	-992.13	87.79
03/01/2014	12	61	1321	60.50	60.33	2.53	15.88	3.32	0.83	1091.34	-1074.81	-189.22
03/01/2014	13	62	1248	61.50	61.33	2.57	16.14	3.58	0.84	1048.43	-950.00	-443.51
03/01/2014	14	63	1318	62.50	62.33	2.61	16.41	3.84	0.85	1124.98	-860.94	-724.13
03/01/2014	15	64	1323	63.50	63.33	2.65	16.67	4.10	0.87	1146.41	-655.79	-940.32
03/01/2014	16	65	1261	64.50	64.32	2.69	16.93	4.37	0.88	1108.40	-376.39	-1042.54
03/01/2014	17	66	1223	65.50	65.32	2.74	17.19	4.63	0.89	1089.59	-91.36	-1085.75
03/01/2014	18	67	1278	66.50	66.32	2.78	17.46	4.89	0.90	1153.14	204.82	-1134.80
03/01/2014	19	68	1286	67.50	67.32	2.82	17.72	5.15	0.91	1174.27	501.32	-1061.88
03/01/2014	20	69	1281	68.50	68.31	2.86	17.98	5.42	0.92	1182.83	765.25	-901.93
03/01/2014	21	70	1339	69.50	69.31	2.90	18.24	5.68	0.93	1249.30	1027.78	-710.23
03/01/2014	22	71	1247	70.50	70.31	2.95	18.51	5.94	0.94	1174.75	1106.65	-394.16
03/01/2014	23	72	1262	71.50	71.30	2.99	18.77	6.20	0.95	1199.51	1195.71	-95.44
04/01/2014	0	73	1275	72.50	72.30	3.03	19.03	0.18	0.96	1221.81	1201.44	222.18
04/01/2014	1	74	1283	73.50	73.30	3.07	19.29	0.45	0.97	1238.66	1117.82	533.62
04/01/2014	2	75	1315	74.50	74.30	3.11	19.56	0.71	0.97	1278.10	971.01	831.07
04/01/2014	3	76	1251	75.50	75.29	3.15	19.82	0.97	0.98	1223.21	691.06	1009.30
04/01/2014	4	77	1318	76.50	76.29	3.20	20.08	1.23	0.98	1295.55	429.44	1222.30
04/01/2014	5	78	1253	77.50	77.29	3.24	20.35	1.50	0.99	1237.29	93.14	1233.78
04/01/2014	6	79	1255	78.50	78.29	3.28	20.61	1.76	0.99	1244.06	-231.49	1222.33
04/01/2014	7	80	1352	79.50	79.28	3.32	20.87	2.02	0.99	1344.45	-584.41	1210.79

04/01/2014	8	81	1295	80.50	80.28	3.36	21.13	2.28	1.00	1290.93	-843.62	977.14
04/01/2014	9	82	1312	81.50	81.28	3.41	21.40	2.55	1.00	1310.17	-1084.22	735.53
04/01/2014	10	83	1253	82.50	82.27	3.45	21.66	2.81	1.00	1252.56	-1183.52	410.11
04/01/2014	11	84	1284	83.50	83.27	3.49	21.92	3.07	1.00	1284.00	-1280.76	91.15
04/01/2014	12	85	1299	84.50	84.27	3.53	22.18	3.33	1.00	1298.55	-1274.82	-247.11
04/01/2014	13	86	1280	85.50	85.27	3.57	22.45	3.60	1.00	1278.21	-1148.74	-560.56
04/01/2014	14	87	1285	86.50	86.26	3.61	22.71	3.86	1.00	1280.96	-965.98	-841.27
04/01/2014	15	88	1217	87.50	87.26	3.66	22.97	4.12	0.99	1210.20	-675.10	-1004.41
04/01/2014	16	89	1337	88.50	88.26	3.70	23.23	4.38	0.99	1325.35	-428.55	-1254.15
04/01/2014	17	90	1333	89.50	89.26	3.74	23.50	4.65	0.99	1316.29	-87.79	-1313.36
04/01/2014	18	91	1377	90.50	90.25	3.78	23.76	4.91	0.98	1353.54	263.29	-1327.69
04/01/2014	19	92	1315	91.50	91.25	3.82	24.02	5.17	0.98	1285.79	568.85	-1153.11
04/01/2014	20	93	1391	92.50	92.25	3.86	24.28	5.43	0.97	1351.97	892.28	-1015.71
04/01/2014	21	94	1411	93.50	93.24	3.91	24.55	5.70	0.97	1362.23	1133.84	-755.04
04/01/2014	22	95	1366	94.50	94.24	3.95	24.81	5.96	0.96	1309.01	1240.50	-417.93
04/01/2014	23	96	1383	95.50	95.24	3.99	25.07	6.22	0.95	1314.52	1311.96	-82.03
05/01/2014	0	97	1322	96.50	96.24	4.03	25.33	0.20	0.94	1245.40	1220.56	247.51
05/01/2014	1	98	1361	97.50	97.23	4.07	25.60	0.46	0.93	1269.83	1136.37	566.68
05/01/2014	2	99	1296	98.50	98.23	4.12	25.86	0.73	0.92	1196.68	895.63	793.65
05/01/2014	3	100	1353	99.50	99.23	4.16	26.12	0.99	0.91	1235.45	680.34	1031.25
05/01/2014	4	101	1345	100.50	100.23	4.20	26.38	1.25	0.90	1213.59	382.52	1151.73
05/01/2014	5	102	1279	101.50	101.22	4.24	26.65	1.51	0.89	1139.48	66.22	1137.56
05/01/2014	6	103	1354	102.50	102.22	4.28	26.91	1.78	0.88	1190.15	-241.54	1165.38
05/01/2014	7	104	1275	103.50	103.22	4.32	27.17	2.04	0.87	1104.82	-497.29	986.58
05/01/2014	8	105	1239	104.50	104.21	4.37	27.43	2.30	0.85	1057.55	-704.78	788.48
05/01/2014	9	106	1267	105.50	105.21	4.41	27.70	2.56	0.84	1064.39	-890.98	582.31
05/01/2014	10	107	1255	106.50	106.21	4.45	27.96	2.83	0.83	1036.81	-985.36	322.56
05/01/2014	11	108	1266	107.50	107.21	4.49	28.22	3.09	0.81	1027.67	-1026.18	55.31
05/01/2014	12	109	1330	108.50	108.20	4.53	28.48	3.35	0.80	1059.89	-1036.90	-219.57
05/01/2014	13	110	1269	109.50	109.20	4.57	28.75	3.61	0.78	991.93	-883.84	-450.28
05/01/2014	14	111	1277	110.50	110.20	4.62	29.01	3.88	0.77	978.20	-726.51	-655.03
05/01/2014	15	112	1230	111.50	111.20	4.66	29.27	4.14	0.75	922.50	-501.36	-774.37
05/01/2014	16	113	1257	112.50	112.19	4.70	29.53	4.40	0.73	922.18	-283.13	-877.64
05/01/2014	17	114	1235	113.50	113.19	4.74	29.80	4.66	0.72	885.42	-43.85	-884.34
05/01/2014	18	115	1274	114.50	114.19	4.78	30.06	4.93	0.70	891.73	188.48	-871.58
05/01/2014	19	116	1282	115.50	115.18	4.83	30.32	5.19	0.68	875.18	400.63	-778.10
05/01/2014	20	117	1223	116.50	116.18	4.87	30.58	5.45	0.67	813.47	547.31	-601.81
05/01/2014	21	118	1310	117.50	117.18	4.91	30.85	5.71	0.65	848.06	713.86	-457.84
05/01/2014	22	119	1282	118.50	118.18	4.95	31.11	5.98	0.63	806.90	768.99	-244.43
05/01/2014	23	120	1276	119.50	119.17	4.99	31.37	6.24	0.61	779.97	779.17	-35.28
06/01/2014	0	121	1236	120.50	120.17	5.03	31.63	0.22	0.59	732.89	715.66	157.99
06/01/2014	1	122	1259	121.50	121.17	5.08	31.90	0.48	0.57	723.32	641.65	333.88
06/01/2014	2	123	1295	122.50	122.17	5.12	32.16	0.74	0.56	720.00	530.57	486.71

06/01/2014	3	124	1296	123.50	123.16	5.16	32.42	1.00	0.54	696.43	373.45	587.83
06/01/2014	4	125	1308	124.50	124.16	5.20	32.68	1.27	0.52	678.45	202.74	647.45
06/01/2014	5	126	1265	125.50	125.16	5.24	32.95	1.53	0.50	632.50	25.89	631.97
06/01/2014	6	127	1242	126.50	126.15	5.29	33.21	1.79	0.48	597.78	-131.37	583.17
06/01/2014	7	128	1228	127.50	127.15	5.33	33.47	2.05	0.46	568.12	-264.40	502.84
06/01/2014	8	129	1311	128.50	128.15	5.37	33.73	2.32	0.44	582.11	-395.34	427.27
06/01/2014	9	130	1225	129.50	129.15	5.41	34.00	2.58	0.43	521.21	-441.13	277.60
06/01/2014	10	131	1242	130.50	130.14	5.45	34.26	2.84	0.41	505.55	-483.09	148.99
06/01/2014	11	132	1334	131.50	131.14	5.49	34.52	3.10	0.39	518.58	-518.23	19.00
06/01/2014	12	133	1256	132.50	132.14	5.54	34.78	3.37	0.37	465.46	-453.64	-104.24
06/01/2014	13	134	1281	133.50	133.14	5.58	35.05	3.63	0.35	451.71	-398.90	-211.94
06/01/2014	14	135	1276	134.50	134.13	5.62	35.31	3.89	0.33	427.28	-312.37	-291.54
06/01/2014	15	136	1274	135.50	135.13	5.66	35.57	4.16	0.32	404.28	-213.85	-343.09
06/01/2014	16	137	1252	136.50	136.13	5.70	35.83	4.42	0.30	375.67	-109.17	-359.46
06/01/2014	17	138	1228	137.50	137.12	5.74	36.10	4.68	0.28	347.60	-11.24	-347.41
06/01/2014	18	139	1315	138.50	138.12	5.79	36.36	4.94	0.27	350.27	79.91	-341.03
06/01/2014	19	140	1358	139.50	139.12	5.83	36.62	5.21	0.25	339.50	160.58	-299.12
06/01/2014	20	141	1422	140.50	140.12	5.87	36.88	5.47	0.23	332.73	228.06	-242.27
06/01/2014	21	142	1366	141.50	141.11	5.91	37.15	5.73	0.22	298.25	253.79	-156.67
06/01/2014	22	143	1254	142.50	142.11	5.95	37.41	5.99	0.20	254.67	244.00	-72.96
06/01/2014	23	144	1349	143.50	143.11	6.00	37.67	6.26	0.19	253.96	253.86	-7.12
07/01/2014	0	145	1341	144.50	144.11	6.04	37.93	0.23	0.17	233.14	226.76	54.17
07/01/2014	1	146	1354	145.50	145.10	6.08	38.20	0.50	0.16	216.52	190.33	103.23
07/01/2014	2	147	1279	146.50	146.10	6.12	38.46	0.76	0.15	187.31	135.83	128.97
07/01/2014	3	148	1238	147.50	147.10	6.16	38.72	1.02	0.13	165.24	86.20	140.98
07/01/2014	4	149	1271	148.50	148.09	6.20	38.98	1.28	0.12	153.81	43.43	147.55
07/01/2014	5	150	1242	149.50	149.09	6.25	39.25	1.55	0.11	135.48	3.22	135.44
07/01/2014	6	151	1242	150.50	150.09	6.29	39.51	1.81	0.10	121.34	-28.70	117.90
07/01/2014	7	152	1233	151.50	151.09	6.33	39.77	2.07	0.09	107.12	-51.48	93.94
07/01/2014	8	153	1240	152.50	152.08	6.37	40.03	2.33	0.08	95.03	-65.73	68.63
07/01/2014	9	154	1295	153.50	153.08	6.41	40.30	2.60	0.07	86.75	-74.20	44.93
07/01/2014	10	155	1249	154.50	154.08	6.46	40.56	2.86	0.06	72.37	-69.51	20.14
07/01/2014	11	156	1243	155.50	155.08	6.50	40.82	3.12	0.05	61.55	-61.54	1.20
07/01/2014	12	157	1268	156.50	156.07	6.54	41.08	3.38	0.04	52.90	-51.34	-12.73
07/01/2014	13	158	1225	157.50	157.07	6.58	41.35	3.65	0.03	42.34	-37.04	-20.51
07/01/2014	14	159	1287	158.50	158.07	6.62	41.61	3.91	0.03	36.11	-25.97	-25.09
07/01/2014	15	160	1203	159.50	159.06	6.66	41.87	4.17	0.02	26.72	-13.74	-22.92
07/01/2014	16	161	1271	160.50	160.06	6.71	42.13	4.43	0.02	21.65	-5.94	-20.82
07/01/2014	17	162	1163	161.50	161.06	6.75	42.40	4.70	0.01	14.58	-0.22	-14.58
07/01/2014	18	163	1242	162.50	162.06	6.79	42.66	4.96	0.01	10.83	2.65	-10.50
07/01/2014	19	164	1258	163.50	163.05	6.83	42.92	5.22	0.01	7.03	3.43	-6.13
07/01/2014	20	165	1287	164.50	164.05	6.87	43.18	5.48	0.00	4.05	2.82	-2.90
07/01/2014	21	166	1242	165.50	165.05	6.91	43.45	5.75	0.00	1.74	1.49	-0.89
07/01/2014	22	167	1224	166.50	166.05	6.96	43.71	6.01	0.00	0.43	0.41	-0.12
07/01/2014	23	168	1247	167.50	167.04	7.00	43.97	6.27	0.00	0.00	0.00	0.00

Sum:	108375	527.28	-1.02
		Deviation(%):	0.49

Using CAST diagram, sum of x is positive and sum of y is negative hence 4th quadrant has excess of cosmic rays

Direction of Source:	Tan (α):	-0.0019
	Alpha, α (Rads):	-0.0019
	Alpha, α (degrees)	-0.1112
	Fraction of Earth Revolution:	0.0003
	Solar Hours after Midnight on First Day of Observation:	0.0074

Table 2. Processed Data for HiSPARC Station 7001, University of Twente, Enschede, Netherlands

Enschede Station 7002 – Processed Data												
Date	Time (hours)	Overall Bin Number	Events (per hour)	Time (solar hours)	Time (sidereal hours)	Number of Earth Revolutions	Angle, α (Rads)	Angle, α (Rads, 0-2π)	Weighting Factor	Weighted Data	Data x (cos)	Data y (sin)
01/01/2014	0	1	1499	0.50	0.50	0.02	0.13	0.13	0.00	0.52	0.52	0.07
01/01/2014	1	2	1446	1.50	1.50	0.06	0.39	0.39	0.00	2.02	1.87	0.78
01/01/2014	2	3	1476	2.50	2.49	0.10	0.66	0.66	0.00	4.64	3.68	2.83
01/01/2014	3	4	1507	3.50	3.49	0.15	0.92	0.92	0.01	8.42	5.11	6.69
01/01/2014	4	5	1384	4.50	4.49	0.19	1.18	1.18	0.01	12.06	4.58	11.16
01/01/2014	5	6	1409	5.50	5.48	0.23	1.44	1.44	0.01	17.66	2.24	17.52
01/01/2014	6	7	1480	6.50	6.48	0.27	1.71	1.71	0.02	25.21	-3.41	24.98
01/01/2014	7	8	1298	7.50	7.48	0.31	1.97	1.97	0.02	28.83	-11.18	26.58
01/01/2014	8	9	1366	8.50	8.48	0.36	2.23	2.23	0.03	38.33	-23.52	30.26
01/01/2014	9	10	1395	9.50	9.47	0.40	2.49	2.49	0.03	48.22	-38.45	29.09
01/01/2014	10	11	1474	10.50	10.47	0.44	2.76	2.76	0.04	61.49	-56.99	23.10
01/01/2014	11	12	1372	11.50	11.47	0.48	3.02	3.02	0.05	67.94	-67.42	8.31
01/01/2014	12	13	1467	12.50	12.47	0.52	3.28	3.28	0.06	85.00	-84.17	-11.85
01/01/2014	13	14	1402	13.50	13.46	0.56	3.54	3.54	0.07	93.92	-86.42	-36.78
01/01/2014	14	15	1458	14.50	14.46	0.61	3.81	3.81	0.08	111.74	-87.94	-68.94
01/01/2014	15	16	1455	15.50	15.46	0.65	4.07	4.07	0.09	126.41	-75.84	-101.14
01/01/2014	16	17	1446	16.50	16.45	0.69	4.33	4.33	0.10	141.28	-52.52	-131.15
01/01/2014	17	18	1526	17.50	17.45	0.73	4.59	4.59	0.11	166.46	-19.66	-165.30
01/01/2014	18	19	1497	18.50	18.45	0.77	4.86	4.86	0.12	181.16	26.03	-179.28
01/01/2014	19	20	1409	19.50	19.45	0.81	5.12	5.12	0.13	188.06	74.39	-172.73
01/01/2014	20	21	1427	20.50	20.44	0.86	5.38	5.38	0.15	208.98	129.64	-163.91
01/01/2014	21	22	1447	21.50	21.44	0.90	5.64	5.64	0.16	231.40	185.73	-138.02
01/01/2014	22	23	1441	22.50	22.44	0.94	5.91	5.91	0.17	250.53	232.97	-92.13
01/01/2014	23	24	1463	23.50	23.44	0.98	6.17	6.17	0.19	275.42	273.63	-31.34
02/01/2014	0	25	1556	24.50	24.43	1.02	6.43	0.15	0.20	316.01	312.53	46.74
02/01/2014	1	26	1540	25.50	25.43	1.07	6.69	0.41	0.22	336.24	308.24	134.33
02/01/2014	2	27	1460	26.50	26.43	1.11	6.96	0.67	0.23	341.62	267.02	213.07
02/01/2014	3	28	1537	27.50	27.42	1.15	7.22	0.94	0.25	384.25	227.86	309.40
02/01/2014	4	29	1538	28.50	28.42	1.19	7.48	1.20	0.27	409.67	149.01	381.61
02/01/2014	5	30	1561	29.50	29.42	1.23	7.74	1.46	0.28	441.85	48.40	439.20
02/01/2014	6	31	1532	30.50	30.42	1.27	8.01	1.72	0.30	459.68	-69.95	454.33
02/01/2014	7	32	1490	31.50	31.41	1.32	8.27	1.99	0.32	472.82	-190.76	432.63
02/01/2014	8	33	1482	32.50	32.41	1.36	8.53	2.25	0.33	496.26	-311.19	386.57
02/01/2014	9	34	1510	33.50	33.41	1.40	8.79	2.51	0.35	532.46	-430.09	313.91
02/01/2014	10	35	1514	34.50	34.41	1.44	9.06	2.77	0.37	561.07	-523.52	201.83
02/01/2014	11	36	1586	35.50	35.40	1.48	9.32	3.04	0.39	616.54	-613.12	64.90
02/01/2014	12	37	1503	36.50	36.40	1.52	9.58	3.30	0.41	611.79	-604.26	-95.69
02/01/2014	13	38	1461	37.50	37.40	1.57	9.84	3.56	0.43	621.62	-567.71	-253.23

02/01/2014	14	39	1507	38.50	38.39	1.61	10.11	3.82	0.44	669.13	-519.42	-421.84
02/01/2014	15	40	1443	39.50	39.39	1.65	10.37	4.09	0.46	667.58	-391.24	-540.92
02/01/2014	16	41	1448	40.50	40.39	1.69	10.63	4.35	0.48	696.93	-247.90	-651.35
02/01/2014	17	42	1440	41.50	41.39	1.73	10.89	4.61	0.50	720.00	-72.71	-716.32
02/01/2014	18	43	1477	42.50	42.38	1.78	11.16	4.87	0.52	766.11	123.09	-756.16
02/01/2014	19	44	1429	43.50	43.38	1.82	11.42	5.14	0.54	767.89	315.83	-699.94
02/01/2014	20	45	1401	44.50	44.38	1.86	11.68	5.40	0.56	778.93	493.65	-602.53
02/01/2014	21	46	1402	45.50	45.38	1.90	11.94	5.66	0.57	805.48	654.68	-469.25
02/01/2014	22	47	1471	46.50	46.37	1.94	12.21	5.92	0.59	872.24	816.52	-306.75
02/01/2014	23	48	1459	47.50	47.37	1.98	12.47	6.19	0.61	891.83	887.65	-86.24
03/01/2014	0	49	1461	48.50	48.37	2.03	12.73	0.17	0.63	919.57	906.98	151.64
03/01/2014	1	50	1458	49.50	49.36	2.07	12.99	0.43	0.65	943.88	858.67	391.91
03/01/2014	2	51	1476	50.50	50.36	2.11	13.26	0.69	0.67	981.75	756.73	625.44
03/01/2014	3	52	1476	51.50	51.36	2.15	13.52	0.95	0.68	1007.62	583.48	821.49
03/01/2014	4	53	1486	52.50	52.36	2.19	13.78	1.22	0.70	1040.12	361.60	975.24
03/01/2014	5	54	1499	53.50	53.35	2.24	14.04	1.48	0.72	1074.70	99.32	1070.10
03/01/2014	6	55	1450	54.50	54.35	2.28	14.31	1.74	0.73	1063.77	-179.93	1048.44
03/01/2014	7	56	1491	55.50	55.35	2.32	14.57	2.00	0.75	1118.25	-468.69	1015.29
03/01/2014	8	57	1518	56.50	56.35	2.36	14.83	2.27	0.77	1162.81	-744.65	893.10
03/01/2014	9	58	1429	57.50	57.34	2.40	15.09	2.53	0.78	1116.99	-913.43	642.89
03/01/2014	10	59	1451	58.50	58.34	2.44	15.36	2.79	0.80	1156.32	-1085.91	397.33
03/01/2014	11	60	1495	59.50	59.34	2.49	15.62	3.05	0.81	1213.56	-1208.84	106.96
03/01/2014	12	61	1517	60.50	60.33	2.53	15.88	3.32	0.83	1253.26	-1234.28	-217.30
03/01/2014	13	62	1491	61.50	61.33	2.57	16.14	3.58	0.84	1252.57	-1134.98	-529.87
03/01/2014	14	63	1479	62.50	62.33	2.61	16.41	3.84	0.85	1262.41	-966.11	-812.59
03/01/2014	15	64	1505	63.50	63.33	2.65	16.67	4.10	0.87	1304.12	-746.00	-1069.68
03/01/2014	16	65	1443	64.50	64.32	2.69	16.93	4.37	0.88	1268.38	-430.71	-1193.01
03/01/2014	17	66	1413	65.50	65.32	2.74	17.19	4.63	0.89	1258.86	-105.56	-1254.43
03/01/2014	18	67	1474	66.50	66.32	2.78	17.46	4.89	0.90	1329.99	236.23	-1308.84
03/01/2014	19	68	1446	67.50	67.32	2.82	17.72	5.15	0.91	1320.37	563.69	-1194.00
03/01/2014	20	69	1369	68.50	68.31	2.86	17.98	5.42	0.92	1264.08	817.82	-963.89
03/01/2014	21	70	1446	69.50	69.31	2.90	18.24	5.68	0.93	1349.14	1109.91	-766.98
03/01/2014	22	71	1396	70.50	70.31	2.95	18.51	5.94	0.94	1315.11	1238.88	-441.26

03/01/2014	23	72	1405	71.50	71.30	2.99	18.77	6.20	0.95	1335.43	1331.20	-106.25
04/01/2014	0	73	1414	72.50	72.30	3.03	19.03	0.18	0.96	1355.01	1332.42	246.41
04/01/2014	1	74	1451	73.50	73.30	3.07	19.29	0.45	0.97	1400.85	1264.19	603.49
04/01/2014	2	75	1410	74.50	74.30	3.11	19.56	0.71	0.97	1370.44	1041.16	891.11
04/01/2014	3	76	1512	75.50	75.29	3.15	19.82	0.97	0.98	1478.41	835.24	1219.87
04/01/2014	4	77	1382	76.50	76.29	3.20	20.08	1.23	0.98	1358.45	450.29	1281.65
04/01/2014	5	78	1393	77.50	77.29	3.24	20.35	1.50	0.99	1375.54	103.55	1371.63
04/01/2014	6	79	1390	78.50	78.29	3.28	20.61	1.76	0.99	1377.88	-256.39	1353.82
04/01/2014	7	80	1386	79.50	79.28	3.32	20.87	2.02	0.99	1378.26	-599.10	1241.24
04/01/2014	8	81	1463	80.50	80.28	3.36	21.13	2.28	1.00	1458.40	-953.07	1103.90
04/01/2014	9	82	1430	81.50	81.28	3.41	21.40	2.55	1.00	1428.00	-1181.73	801.68
04/01/2014	10	83	1456	82.50	82.27	3.45	21.66	2.81	1.00	1455.49	-1375.27	476.55
04/01/2014	11	84	1379	83.50	83.27	3.49	21.92	3.07	1.00	1379.00	-1375.52	97.89
04/01/2014	12	85	1437	84.50	84.27	3.53	22.18	3.33	1.00	1436.50	-1410.25	-273.37
04/01/2014	13	86	1417	85.50	85.27	3.57	22.45	3.60	1.00	1415.02	-1271.69	-620.56
04/01/2014	14	87	1442	86.50	86.26	3.61	22.71	3.86	1.00	1437.47	-1084.01	-944.06
04/01/2014	15	88	1455	87.50	87.26	3.66	22.97	4.12	0.99	1446.87	-807.12	-1200.83
04/01/2014	16	89	1522	88.50	88.26	3.70	23.23	4.38	0.99	1508.73	-487.84	-1427.68
04/01/2014	17	90	1548	89.50	89.26	3.74	23.50	4.65	0.99	1528.59	-101.95	-1525.19
04/01/2014	18	91	1464	90.50	90.25	3.78	23.76	4.91	0.98	1439.06	279.93	-1411.57
04/01/2014	19	92	1484	91.50	91.25	3.82	24.02	5.17	0.98	1451.04	641.95	-1301.31
04/01/2014	20	93	1481	92.50	92.25	3.86	24.28	5.43	0.97	1439.45	950.01	-1081.42
04/01/2014	21	94	1516	93.50	93.24	3.91	24.55	5.70	0.97	1463.60	1218.22	-811.22
04/01/2014	22	95	1451	94.50	94.24	3.95	24.81	5.96	0.96	1390.47	1317.69	-443.94
04/01/2014	23	96	1467	95.50	95.24	3.99	25.07	6.22	0.95	1394.36	1391.64	-87.02
05/01/2014	0	97	1385	96.50	96.24	4.03	25.33	0.20	0.94	1304.75	1278.72	259.30
05/01/2014	1	98	1475	97.50	97.23	4.07	25.60	0.46	0.93	1376.19	1231.56	614.14
05/01/2014	2	99	1509	98.50	98.23	4.12	25.86	0.73	0.92	1393.35	1042.83	924.09

05/01/2014	3	100	1509	99.50	99.23	4.16	26.12	0.99	0.91	1377.90	758.78	1150.15
05/01/2014	4	101	1499	100.50	100.23	4.20	26.38	1.25	0.90	1352.55	426.32	1283.60
05/01/2014	5	102	1439	101.50	101.22	4.24	26.65	1.51	0.89	1282.03	74.50	1279.86
05/01/2014	6	103	1428	102.50	102.22	4.28	26.91	1.78	0.88	1255.19	-254.74	1229.07
05/01/2014	7	104	1474	103.50	103.22	4.32	27.17	2.04	0.87	1277.26	-574.90	1140.56
05/01/2014	8	105	1400	104.50	104.21	4.37	27.43	2.30	0.85	1194.97	-796.36	890.94
05/01/2014	9	106	1440	105.50	105.21	4.41	27.70	2.56	0.84	1209.72	-1012.63	661.82
05/01/2014	10	107	1364	106.50	106.21	4.45	27.96	2.83	0.83	1126.86	-1070.94	350.58
05/01/2014	11	108	1362	107.50	107.21	4.49	28.22	3.09	0.81	1105.60	-1103.99	59.50
05/01/2014	12	109	1386	108.50	108.20	4.53	28.48	3.35	0.80	1104.52	-1080.56	-228.81
05/01/2014	13	110	1371	109.50	109.20	4.57	28.75	3.61	0.78	1071.66	-954.88	-486.47
05/01/2014	14	111	1372	110.50	110.20	4.62	29.01	3.88	0.77	1050.97	-780.56	-703.76
05/01/2014	15	112	1392	111.50	111.20	4.66	29.27	4.14	0.75	1044.00	-567.39	-876.36
05/01/2014	16	113	1416	112.50	112.19	4.70	29.53	4.40	0.73	1038.83	-318.94	-988.65
05/01/2014	17	114	1390	113.50	113.19	4.74	29.80	4.66	0.72	996.55	-49.35	-995.33
05/01/2014	18	115	1394	114.50	114.19	4.78	30.06	4.93	0.70	975.72	206.23	-953.68
05/01/2014	19	116	1426	115.50	115.18	4.83	30.32	5.19	0.68	973.49	445.64	-865.50
05/01/2014	20	117	1390	116.50	116.18	4.87	30.58	5.45	0.67	924.54	622.04	-683.99
05/01/2014	21	118	1431	117.50	117.18	4.91	30.85	5.71	0.65	926.40	779.80	-500.13
05/01/2014	22	119	1450	118.50	118.18	4.95	31.11	5.98	0.63	912.64	869.76	-276.46
05/01/2014	23	120	1407	119.50	119.17	4.99	31.37	6.24	0.61	860.04	859.16	-38.90
06/01/2014	0	121	1405	120.50	120.17	5.03	31.63	0.22	0.59	833.10	813.52	179.59
06/01/2014	1	122	1433	121.50	121.17	5.08	31.90	0.48	0.57	823.29	730.33	380.02
06/01/2014	2	123	1504	122.50	122.17	5.12	32.16	0.74	0.56	836.20	616.20	565.26
06/01/2014	3	124	1432	123.50	123.16	5.16	32.42	1.00	0.54	769.51	412.64	649.51
06/01/2014	4	125	1453	124.50	124.16	5.20	32.68	1.27	0.52	753.66	225.21	719.23
06/01/2014	5	126	1437	125.50	125.16	5.24	32.95	1.53	0.50	718.50	29.41	717.90
06/01/2014	6	127	1422	126.50	126.15	5.29	33.21	1.79	0.48	684.41	-150.41	667.68
06/01/2014	7	128	1450	127.50	127.15	5.33	33.47	2.05	0.46	670.82	-312.20	593.74
06/01/2014	8	129	1446	128.50	128.15	5.37	33.73	2.32	0.44	642.05	-436.05	471.26
06/01/2014	9	130	1423	129.50	129.15	5.41	34.00	2.58	0.43	605.46	-512.44	322.47
06/01/2014	10	131	1361	130.50	130.14	5.45	34.26	2.84	0.41	553.99	-529.38	163.27
06/01/2014	11	132	1401	131.50	131.14	5.49	34.52	3.10	0.39	544.62	-544.26	19.95
06/01/2014	12	133	1453	132.50	132.14	5.54	34.78	3.37	0.37	538.47	-524.79	-120.59
06/01/2014	13	134	1397	133.50	133.14	5.58	35.05	3.63	0.35	492.61	-435.02	-231.14
06/01/2014	14	135	1455	134.50	134.13	5.62	35.31	3.89	0.33	487.22	-356.19	-332.43
06/01/2014	15	136	1421	135.50	135.13	5.66	35.57	4.16	0.32	450.93	-238.52	-382.68
06/01/2014	16	137	1440	136.50	136.13	5.70	35.83	4.42	0.30	432.08	-125.56	-413.43

06/01/2014	17	138	1362	137.50	137.12	5.74	36.10	4.68	0.28	385.53	-12.47	-385.32
06/01/2014	18	139	1507	138.50	138.12	5.79	36.36	4.94	0.27	401.41	91.58	-390.83
06/01/2014	19	140	1439	139.50	139.12	5.83	36.62	5.21	0.25	359.75	170.16	-316.96
06/01/2014	20	141	1432	140.50	140.12	5.87	36.88	5.47	0.23	335.07	229.67	-243.97
06/01/2014	21	142	1484	141.50	141.11	5.91	37.15	5.73	0.22	324.02	275.71	-170.21
06/01/2014	22	143	1458	142.50	142.11	5.95	37.41	5.99	0.20	296.11	283.69	-84.83
06/01/2014	23	144	1413	143.50	143.11	6.00	37.67	6.26	0.19	266.00	265.90	-7.46
07/01/2014	0	145	1371	144.50	144.11	6.04	37.93	0.23	0.17	238.36	231.83	55.38
07/01/2014	1	146	1359	145.50	145.10	6.08	38.20	0.50	0.16	217.32	191.03	103.62
07/01/2014	2	147	1390	146.50	146.10	6.12	38.46	0.76	0.15	203.56	147.62	140.16
07/01/2014	3	148	1366	147.50	147.10	6.16	38.72	1.02	0.13	182.33	95.11	155.55
07/01/2014	4	149	1334	148.50	148.09	6.20	38.98	1.28	0.12	161.43	45.58	154.86
07/01/2014	5	150	1415	149.50	149.09	6.25	39.25	1.55	0.11	154.35	3.66	154.31
07/01/2014	6	151	1371	150.50	150.09	6.29	39.51	1.81	0.10	133.95	-31.68	130.15
07/01/2014	7	152	1392	151.50	151.09	6.33	39.77	2.07	0.09	120.94	-58.12	106.06
07/01/2014	8	153	1398	152.50	152.08	6.37	40.03	2.33	0.08	107.14	-74.11	77.38
07/01/2014	9	154	1351	153.50	153.08	6.41	40.30	2.60	0.07	90.50	-77.41	46.88
07/01/2014	10	155	1369	154.50	154.08	6.46	40.56	2.86	0.06	79.32	-76.19	22.07
07/01/2014	11	156	1348	155.50	155.08	6.50	40.82	3.12	0.05	66.75	-66.73	1.30
07/01/2014	12	157	1393	156.50	156.07	6.54	41.08	3.38	0.04	58.11	-56.41	-13.99
07/01/2014	13	158	1448	157.50	157.07	6.58	41.35	3.65	0.03	50.05	-43.79	-24.24
07/01/2014	14	159	1421	158.50	158.07	6.62	41.61	3.91	0.03	39.87	-28.68	-27.70
07/01/2014	15	160	1379	159.50	159.06	6.66	41.87	4.17	0.02	30.63	-15.75	-26.27
07/01/2014	16	161	1364	160.50	160.06	6.71	42.13	4.43	0.02	23.24	-6.37	-22.35
07/01/2014	17	162	1461	161.50	161.06	6.75	42.40	4.70	0.01	18.32	-0.28	-18.31
07/01/2014	18	163	1394	162.50	162.06	6.79	42.66	4.96	0.01	12.15	2.98	-11.78
07/01/2014	19	164	1346	163.50	163.05	6.83	42.92	5.22	0.01	7.52	3.67	-6.56
07/01/2014	20	165	1403	164.50	164.05	6.87	43.18	5.48	0.00	4.41	3.08	-3.16
07/01/2014	21	166	1362	165.50	165.05	6.91	43.45	5.75	0.00	1.90	1.64	-0.97
07/01/2014	22	167	1372	166.50	166.05	6.96	43.71	6.01	0.00	0.48	0.46	-0.13
07/01/2014	23	168	1320	167.50	167.04	7.00	43.97	6.27	0.00	0.00	0.00	0.00

Sum:	121436.82	151.27	117.84
Deviation (%):			0.16

Using CAST diagram, sum of x is positive and sum of y is positive hence 1st quadrant has excess of cosmic rays

Direction of Source:	Tan (α):	0.7790
	Alpha, α (Rads):	0.6618
	Alpha, α (degrees)	37.9190
	Fraction of Earth Revolution:	0.1053
	Solar Hours after Midnight on First Day of Observation:	2.5279

Table 3. Processed Data for HiSPARC Station 7002, University of Twente, Enschede, Netherlands

Enschede Station 7003 – Processed Data

Date	Time (hours)	Overall Bin Number	Events (per hour)	Time (solar hours)	Time (sidereal hours)	Number of Earth Revolutions	Angle, α (Rads)	Angle, α (Rads, 0-2π)	Weighting Factor	Weighted Data	Data x (cos)	Data y (sin)
01/01/2014	0	1	1444	0.50	0.50	0.02	0.13	0.13	0.00	0.50	0.50	0.07
01/01/2014	1	2	1582	1.50	1.50	0.06	0.39	0.39	0.00	2.21	2.04	0.85
01/01/2014	2	3	1461	2.50	2.49	0.10	0.66	0.66	0.00	4.59	3.64	2.80
01/01/2014	3	4	1496	3.50	3.49	0.15	0.92	0.92	0.01	8.35	5.07	6.64
01/01/2014	4	5	1484	4.50	4.49	0.19	1.18	1.18	0.01	12.94	4.91	11.97
01/01/2014	5	6	1414	5.50	5.48	0.23	1.44	1.44	0.01	17.73	2.24	17.58
01/01/2014	6	7	1516	6.50	6.48	0.27	1.71	1.71	0.02	25.83	-3.49	25.59
01/01/2014	7	8	1486	7.50	7.48	0.31	1.97	1.97	0.02	33.01	-12.80	30.43
01/01/2014	8	9	1544	8.50	8.48	0.36	2.23	2.23	0.03	43.32	-26.58	34.21
01/01/2014	9	10	1413	9.50	9.47	0.40	2.49	2.49	0.03	48.84	-38.95	29.47
01/01/2014	10	11	1480	10.50	10.47	0.44	2.76	2.76	0.04	61.74	-57.22	23.20
01/01/2014	11	12	1415	11.50	11.47	0.48	3.02	3.02	0.05	70.06	-69.54	8.57
01/01/2014	12	13	1428	12.50	12.47	0.52	3.28	3.28	0.06	82.74	-81.93	-11.53
01/01/2014	13	14	1449	13.50	13.46	0.56	3.54	3.54	0.07	97.06	-89.31	-38.01
01/01/2014	14	15	1487	14.50	14.46	0.61	3.81	3.81	0.08	113.96	-89.69	-70.31
01/01/2014	15	16	1471	15.50	15.46	0.65	4.07	4.07	0.09	127.80	-76.67	-102.25
01/01/2014	16	17	1469	16.50	16.45	0.69	4.33	4.33	0.10	143.52	-53.35	-133.24
01/01/2014	17	18	1468	17.50	17.45	0.73	4.59	4.59	0.11	160.14	-18.91	-159.02
01/01/2014	18	19	1545	18.50	18.45	0.77	4.86	4.86	0.12	186.97	26.86	-185.03
01/01/2014	19	20	1548	19.50	19.45	0.81	5.12	5.12	0.13	206.62	81.73	-189.77
01/01/2014	20	21	1496	20.50	20.44	0.86	5.38	5.38	0.15	219.08	135.91	-171.83
01/01/2014	21	22	1485	21.50	21.44	0.90	5.64	5.64	0.16	237.47	190.60	-141.64
01/01/2014	22	23	1530	22.50	22.44	0.94	5.91	5.91	0.17	266.00	247.36	-97.82
01/01/2014	23	24	1525	23.50	23.44	0.98	6.17	6.17	0.19	287.09	285.22	-32.67
02/01/2014	0	25	1520	24.50	24.43	1.02	6.43	0.15	0.20	308.70	305.30	45.66
02/01/2014	1	26	1519	25.50	25.43	1.07	6.69	0.41	0.22	331.66	304.04	132.50
02/01/2014	2	27	1527	26.50	26.43	1.11	6.96	0.67	0.23	357.29	279.28	222.85
02/01/2014	3	28	1475	27.50	27.42	1.15	7.22	0.94	0.25	368.75	218.67	296.92
02/01/2014	4	29	1520	28.50	28.42	1.19	7.48	1.20	0.27	404.88	147.27	377.14
02/01/2014	5	30	1569	29.50	29.42	1.23	7.74	1.46	0.28	444.12	48.65	441.45
02/01/2014	6	31	1570	30.50	30.42	1.27	8.01	1.72	0.30	471.08	-71.68	465.60
02/01/2014	7	32	1552	31.50	31.41	1.32	8.27	1.99	0.32	492.50	-198.69	450.64
02/01/2014	8	33	1531	32.50	32.41	1.36	8.53	2.25	0.33	512.67	-321.48	399.35
02/01/2014	9	34	1485	33.50	33.41	1.40	8.79	2.51	0.35	523.64	-422.97	308.71
02/01/2014	10	35	1499	34.50	34.41	1.44	9.06	2.77	0.37	555.52	-518.33	199.83
02/01/2014	11	36	1474	35.50	35.40	1.48	9.32	3.04	0.39	573.00	-569.82	60.31
02/01/2014	12	37	1604	36.50	36.40	1.52	9.58	3.30	0.41	652.90	-644.86	-102.12
02/01/2014	13	38	1500	37.50	37.40	1.57	9.84	3.56	0.43	638.22	-582.86	-259.99

02/01/2014	14	39	1491	38.50	38.39	1.61	10.11	3.82	0.44	662.03	-513.90	-417.36
02/01/2014	15	40	1472	39.50	39.39	1.65	10.37	4.09	0.46	681.00	-399.10	-551.79
02/01/2014	16	41	1507	40.50	40.39	1.69	10.63	4.35	0.48	725.33	-258.00	-677.89
02/01/2014	17	42	1445	41.50	41.39	1.73	10.89	4.61	0.50	722.50	-72.96	-718.81
02/01/2014	18	43	1480	42.50	42.38	1.78	11.16	4.87	0.52	767.67	123.34	-757.70
02/01/2014	19	44	1454	43.50	43.38	1.82	11.42	5.14	0.54	781.33	321.36	-712.18
02/01/2014	20	45	1450	44.50	44.38	1.86	11.68	5.40	0.56	806.17	510.92	-623.60
02/01/2014	21	46	1472	45.50	45.38	1.90	11.94	5.66	0.57	845.70	687.37	-492.68
02/01/2014	22	47	1494	46.50	46.37	1.94	12.21	5.92	0.59	885.88	829.29	-311.55
02/01/2014	23	48	1473	47.50	47.37	1.98	12.47	6.19	0.61	900.39	896.17	-87.07
03/01/2014	0	49	1560	48.50	48.37	2.03	12.73	0.17	0.63	981.88	968.44	161.92
03/01/2014	1	50	1469	49.50	49.36	2.07	12.99	0.43	0.65	951.00	865.14	394.87
03/01/2014	2	51	1522	50.50	50.36	2.11	13.26	0.69	0.67	1012.34	780.32	644.94
03/01/2014	3	52	1418	51.50	51.36	2.15	13.52	0.95	0.68	968.03	560.55	789.21
03/01/2014	4	53	1525	52.50	52.36	2.19	13.78	1.22	0.70	1067.42	371.09	1000.84
03/01/2014	5	54	1508	53.50	53.35	2.24	14.04	1.48	0.72	1081.15	99.92	1076.52
03/01/2014	6	55	1514	54.50	54.35	2.28	14.31	1.74	0.73	1110.72	-187.88	1094.72
03/01/2014	7	56	1473	55.50	55.35	2.32	14.57	2.00	0.75	1104.75	-463.03	1003.03
03/01/2014	8	57	1452	56.50	56.35	2.36	14.83	2.27	0.77	1112.26	-712.27	854.27
03/01/2014	9	58	1557	57.50	57.34	2.40	15.09	2.53	0.78	1217.04	-995.25	700.48
03/01/2014	10	59	1500	58.50	58.34	2.44	15.36	2.79	0.80	1195.37	-1122.58	410.75
03/01/2014	11	60	1483	59.50	59.34	2.49	15.62	3.05	0.81	1203.82	-1199.13	106.10
03/01/2014	12	61	1479	60.50	60.33	2.53	15.88	3.32	0.83	1221.87	-1203.36	-211.85
03/01/2014	13	62	1495	61.50	61.33	2.57	16.14	3.58	0.84	1255.93	-1138.02	-531.29
03/01/2014	14	63	1529	62.50	62.33	2.61	16.41	3.84	0.85	1305.08	-998.77	-840.06
03/01/2014	15	64	1511	63.50	63.33	2.65	16.67	4.10	0.87	1309.32	-748.98	-1073.94
03/01/2014	16	65	1499	64.50	64.32	2.69	16.93	4.37	0.88	1317.60	-447.43	-1239.31
03/01/2014	17	66	1520	65.50	65.32	2.74	17.19	4.63	0.89	1354.19	-113.55	-1349.42
03/01/2014	18	67	1462	66.50	66.32	2.78	17.46	4.89	0.90	1319.16	234.31	-1298.19
03/01/2014	19	68	1417	67.50	67.32	2.82	17.72	5.15	0.91	1293.89	552.39	-1170.05
03/01/2014	20	69	1477	68.50	68.31	2.86	17.98	5.42	0.92	1363.81	882.34	-1039.93
03/01/2014	21	70	1460	69.50	69.31	2.90	18.24	5.68	0.93	1362.20	1120.66	-774.41
03/01/2014	22	71	1474	70.50	70.31	2.95	18.51	5.94	0.94	1388.59	1308.10	-465.91
03/01/2014	23	72	1517	71.50	71.30	2.99	18.77	6.20	0.95	1441.88	1437.31	-114.72
04/01/2014	0	73	1397	72.50	72.30	3.03	19.03	0.18	0.96	1338.72	1316.40	243.44
04/01/2014	1	74	1470	73.50	73.30	3.07	19.29	0.45	0.97	1419.19	1280.74	611.39
04/01/2014	2	75	1385	74.50	74.30	3.11	19.56	0.71	0.97	1346.14	1022.70	875.31
04/01/2014	3	76	1439	75.50	75.29	3.15	19.82	0.97	0.98	1407.03	794.91	1160.97
04/01/2014	4	77	1410	76.50	76.29	3.20	20.08	1.23	0.98	1385.98	459.42	1307.62
04/01/2014	5	78	1475	77.50	77.29	3.24	20.35	1.50	0.99	1456.51	109.64	1452.38
04/01/2014	6	79	1408	78.50	78.29	3.28	20.61	1.76	0.99	1395.73	-259.71	1371.35
04/01/2014	7	80	1478	79.50	79.28	3.32	20.87	2.02	0.99	1469.75	-638.87	1323.63
04/01/2014	8	81	1464	80.50	80.28	3.36	21.13	2.28	1.00	1459.40	-953.72	1104.66
04/01/2014	9	82	1462	81.50	81.28	3.41	21.40	2.55	1.00	1459.96	-1208.18	819.62
04/01/2014	10	83	1481	82.50	82.27	3.45	21.66	2.81	1.00	1480.48	-1398.88	484.73

04/01/2014	11	84	1497	83.50	83.27	3.49	21.92	3.07	1.00	1497.00	-1493.22	106.27
04/01/2014	12	85	1538	84.50	84.27	3.53	22.18	3.33	1.00	1537.46	-1509.37	-292.58
04/01/2014	13	86	1549	85.50	85.27	3.57	22.45	3.60	1.00	1546.83	-1390.15	-678.36
04/01/2014	14	87	1514	86.50	86.26	3.61	22.71	3.86	1.00	1509.24	-1138.13	-991.19
04/01/2014	15	88	1489	87.50	87.26	3.66	22.97	4.12	0.99	1480.68	-825.98	-1228.89
04/01/2014	16	89	1506	88.50	88.26	3.70	23.23	4.38	0.99	1492.87	-482.72	-1412.68
04/01/2014	17	90	1540	89.50	89.26	3.74	23.50	4.65	0.99	1520.69	-101.43	-1517.31
04/01/2014	18	91	1537	90.50	90.25	3.78	23.76	4.91	0.98	1510.81	293.88	-1481.96
04/01/2014	19	92	1498	91.50	91.25	3.82	24.02	5.17	0.98	1464.72	648.01	-1313.58
04/01/2014	20	93	1514	92.50	92.25	3.86	24.28	5.43	0.97	1471.52	971.18	-1105.52
04/01/2014	21	94	1525	93.50	93.24	3.91	24.55	5.70	0.97	1472.29	1225.45	-816.04
04/01/2014	22	95	1605	94.50	94.24	3.95	24.81	5.96	0.96	1538.04	1457.54	-491.06
04/01/2014	23	96	1568	95.50	95.24	3.99	25.07	6.22	0.95	1490.36	1487.45	-93.01
05/01/2014	0	97	1511	96.50	96.24	4.03	25.33	0.20	0.94	1423.45	1395.06	282.89
05/01/2014	1	98	1496	97.50	97.23	4.07	25.60	0.46	0.93	1395.79	1249.09	622.89
05/01/2014	2	99	1551	98.50	98.23	4.12	25.86	0.73	0.92	1432.13	1071.86	949.81
05/01/2014	3	100	1536	99.50	99.23	4.16	26.12	0.99	0.91	1402.55	772.36	1170.73
05/01/2014	4	101	1537	100.50	100.23	4.20	26.38	1.25	0.90	1386.83	437.12	1316.14
05/01/2014	5	102	1479	101.50	101.22	4.24	26.65	1.51	0.89	1317.66	76.57	1315.44
05/01/2014	6	103	1506	102.50	102.22	4.28	26.91	1.78	0.88	1323.75	-268.66	1296.20
05/01/2014	7	104	1501	103.50	103.22	4.32	27.17	2.04	0.87	1300.66	-585.44	1161.45
05/01/2014	8	105	1509	104.50	104.21	4.37	27.43	2.30	0.85	1288.01	-858.36	960.31
05/01/2014	9	106	1466	105.50	105.21	4.41	27.70	2.56	0.84	1231.57	-1030.92	673.77
05/01/2014	10	107	1384	106.50	106.21	4.45	27.96	2.83	0.83	1143.38	-1086.64	355.72
05/01/2014	11	108	1423	107.50	107.21	4.49	28.22	3.09	0.81	1155.11	-1153.44	62.17
05/01/2014	12	109	1449	108.50	108.20	4.53	28.48	3.35	0.80	1154.72	-1129.67	-239.21
05/01/2014	13	110	1450	109.50	109.20	4.57	28.75	3.61	0.78	1133.41	-1009.90	-514.50
05/01/2014	14	111	1438	110.50	110.20	4.62	29.01	3.88	0.77	1101.53	-818.11	-737.61
05/01/2014	15	112	1446	111.50	111.20	4.66	29.27	4.14	0.75	1084.50	-589.40	-910.35
05/01/2014	16	113	1414	112.50	112.19	4.70	29.53	4.40	0.73	1037.36	-318.49	-987.26
05/01/2014	17	114	1396	113.50	113.19	4.74	29.80	4.66	0.72	1000.85	-49.57	-999.62
05/01/2014	18	115	1497	114.50	114.19	4.78	30.06	4.93	0.70	1047.82	221.47	-1024.15
05/01/2014	19	116	1454	115.50	115.18	4.83	30.32	5.19	0.68	992.60	454.39	-882.49
05/01/2014	20	117	1502	116.50	116.18	4.87	30.58	5.45	0.67	999.04	672.17	-739.10
05/01/2014	21	118	1499	117.50	117.18	4.91	30.85	5.71	0.65	970.42	816.85	-523.90
05/01/2014	22	119	1453	118.50	118.18	4.95	31.11	5.98	0.63	914.53	871.56	-277.03
05/01/2014	23	120	1405	119.50	119.17	4.99	31.37	6.24	0.61	858.82	857.94	-38.84
06/01/2014	0	121	1472	120.50	120.17	5.03	31.63	0.22	0.59	872.83	852.31	188.15
06/01/2014	1	122	1463	121.50	121.17	5.08	31.90	0.48	0.57	840.52	745.62	387.98
06/01/2014	2	123	1464	122.50	122.17	5.12	32.16	0.74	0.56	813.96	599.82	550.23
06/01/2014	3	124	1528	123.50	123.16	5.16	32.42	1.00	0.54	821.09	440.30	693.06
06/01/2014	4	125	1504	124.50	124.16	5.20	32.68	1.27	0.52	780.12	233.12	744.47
06/01/2014	5	126	1457	125.50	125.16	5.24	32.95	1.53	0.50	728.50	29.82	727.89
06/01/2014	6	127	1448	126.50	126.15	5.29	33.21	1.79	0.48	696.93	-153.16	679.89
06/01/2014	7	128	1544	127.50	127.15	5.33	33.47	2.05	0.46	714.31	-332.44	632.23

06/01/2014	8	129	1418	128.50	128.15	5.37	33.73	2.32	0.44	629.62	-427.61	462.14
06/01/2014	9	130	1491	129.50	129.15	5.41	34.00	2.58	0.43	634.39	-536.92	337.88
06/01/2014	10	131	1431	130.50	130.14	5.45	34.26	2.84	0.41	582.48	-556.61	171.67
06/01/2014	11	132	1413	131.50	131.14	5.49	34.52	3.10	0.39	549.29	-548.92	20.12
06/01/2014	12	133	1437	132.50	132.14	5.54	34.78	3.37	0.37	532.54	-519.01	-119.27
06/01/2014	13	134	1488	133.50	133.14	5.58	35.05	3.63	0.35	524.70	-463.36	-246.19
06/01/2014	14	135	1525	134.50	134.13	5.62	35.31	3.89	0.33	510.66	-373.33	-348.43
06/01/2014	15	136	1508	135.50	135.13	5.66	35.57	4.16	0.32	478.53	-253.12	-406.11
06/01/2014	16	137	1513	136.50	136.13	5.70	35.83	4.42	0.30	453.98	-131.93	-434.39
06/01/2014	17	138	1449	137.50	137.12	5.74	36.10	4.68	0.28	410.15	-13.26	-409.94
06/01/2014	18	139	1488	138.50	138.12	5.79	36.36	4.94	0.27	396.35	90.43	-385.90
06/01/2014	19	140	1536	139.50	139.12	5.83	36.62	5.21	0.25	384.00	181.63	-338.33
06/01/2014	20	141	1566	140.50	140.12	5.87	36.88	5.47	0.23	366.42	251.16	-266.80
06/01/2014	21	142	1589	141.50	141.11	5.91	37.15	5.73	0.22	346.94	295.22	-182.25
06/01/2014	22	143	1467	142.50	142.11	5.95	37.41	5.99	0.20	297.93	285.44	-85.35
06/01/2014	23	144	1455	143.50	143.11	6.00	37.67	6.26	0.19	273.91	273.80	-7.68
07/01/2014	0	145	1446	144.50	144.11	6.04	37.93	0.23	0.17	251.40	244.52	58.41
07/01/2014	1	146	1525	145.50	145.10	6.08	38.20	0.50	0.16	243.87	214.37	116.27
07/01/2014	2	147	1476	146.50	146.10	6.12	38.46	0.76	0.15	216.16	156.75	148.84
07/01/2014	3	148	1459	147.50	147.10	6.16	38.72	1.02	0.13	194.74	101.58	166.14
07/01/2014	4	149	1432	148.50	148.09	6.20	38.98	1.28	0.12	173.29	48.93	166.24
07/01/2014	5	150	1483	149.50	149.09	6.25	39.25	1.55	0.11	161.77	3.84	161.73
07/01/2014	6	151	1465	150.50	150.09	6.29	39.51	1.81	0.10	143.13	-33.85	139.07
07/01/2014	7	152	1472	151.50	151.09	6.33	39.77	2.07	0.09	127.89	-61.46	112.15
07/01/2014	8	153	1403	152.50	152.08	6.37	40.03	2.33	0.08	107.52	-74.37	77.65
07/01/2014	9	154	1508	153.50	153.08	6.41	40.30	2.60	0.07	101.02	-86.41	52.32
07/01/2014	10	155	1437	154.50	154.08	6.46	40.56	2.86	0.06	83.26	-79.98	23.17
07/01/2014	11	156	1453	155.50	155.08	6.50	40.82	3.12	0.05	71.95	-71.93	1.40
07/01/2014	12	157	1442	156.50	156.07	6.54	41.08	3.38	0.04	60.16	-58.39	-14.48
07/01/2014	13	158	1366	157.50	157.07	6.58	41.35	3.65	0.03	47.21	-41.31	-22.87
07/01/2014	14	159	1453	158.50	158.07	6.62	41.61	3.91	0.03	40.77	-29.32	-28.33
07/01/2014	15	160	1452	159.50	159.06	6.66	41.87	4.17	0.02	32.25	-16.59	-27.66
07/01/2014	16	161	1430	160.50	160.06	6.71	42.13	4.43	0.02	24.36	-6.68	-23.43
07/01/2014	17	162	1452	161.50	161.06	6.75	42.40	4.70	0.01	18.20	-0.28	-18.20
07/01/2014	18	163	1408	162.50	162.06	6.79	42.66	4.96	0.01	12.27	3.01	-11.90
07/01/2014	19	164	1427	163.50	163.05	6.83	42.92	5.22	0.01	7.97	3.89	-6.96
07/01/2014	20	165	1407	164.50	164.05	6.87	43.18	5.48	0.00	4.42	3.09	-3.17
07/01/2014	21	166	1365	165.50	165.05	6.91	43.45	5.75	0.00	1.91	1.64	-0.97
07/01/2014	22	167	1411	166.50	166.05	6.96	43.71	6.01	0.00	0.49	0.48	-0.13
07/01/2014	23	168	1365	167.50	167.04	7.00	43.97	6.27	0.00	0.00	0.00	0.00
									Sum:	124824	170.29	-161.93
										Deviation (%):		0.19

Using CAST diagram, sum of x is positive and sum of y is negative hence 4th quadrant has excess of cosmic rays

Direction of Source:	Tan (α):	-0.95
	Alpha, α (Rads):	-0.76
	Alpha, α (degrees):	-43.56
	Fraction of Earth Revolution:	0.12
	Solar Hours after Midnight on First Day of Observation:	2.90

Table 4. Processed Data for HiSPARC Station 7003, University of Twente, Enschede, Netherlands